Rhinology Online

ORIGINAL CONTRIBUTION

OPEN ACCESS

A new computed tomography protocol to assess the olfactory cleft*

Tiago V. Souza[1,2], Roberto E.S. Guimarães[1,2], Alexandre V. Giannetti[2], Caroline S. Caixeta[1], Luís O.G. Vasconcelos[1], Gabriela G. Freitas[1]

[1] Department of Otolaryngology, Mater Dei Hospital, Belo Horizonte, Minas Gerais, Brazil

[2] Department of Otolaryngology, Hospital das Clínicas da Universidade Federal de Minas Gerais, Belo Horizonte, Minas Gerais, Brazil

Rhinology Online, Vol 6: 38 - 45, 2023

http://doi.org/10.4193/RHINOL/22.012

***Received for publication:**

June 3, 2023

Accepted: October 31, 2023

Published: November 8 , 2023

Abstract

Introduction: The olfactory cleft is a region of significant importance within the nasal cavity, given the heightened focus on olfactory disorders in recent years. It is considered a 3-dimensional space that starts at the most anterior olfactory filament and ends just anteriorly to the sphenoid sinus. This study aimed to outline the profile of the olfactory cleft as an anatomical area of extreme relevance in the diagnosis of diseases of the nose, paranasal sinuses and olfactory disorders. The aim to establish parameters of radiological normality for the olfactory cleft enables us to recognize and differentiate nasal disorders by identifying the widening or narrowing of the olfactory cleft during the preoperative assessment, thus facilitating the planning of the optimal treatment. This supports a theory about the evolution and development of the nose (Evo Devo Theory) that shows the olfactory nose (ethmoid and olfactory cleft) represents the seat of most diseases of the nose and paranasal sinuses.

Materials and methods: 700 random CT scans of the nose and sinuses have been studied. A homogeneous group of CT scans of patients without paranasal sinus diseases were included in this study, seeking to define a reference anatomical measure as a criterion for tomographic normality. Measurements of the olfactory cleft were taken in the lateral-lateral direction between the middle concha and the septum on each side of the nose cavity at three specific anatomical points in the anterior skull base in the anteroposterior direction, corresponding to the beginning, middle and end of the olfactory cleft. For data analysis, exploratory statistical techniques have been used that allowed a better visualization of the general characteristics of the data. The appropriate statstical analysis was performed using Statistical Package for Social Sciences (SPSS).

Results: According to the statistical analysis performed, the reference values that were found evaluating and studying the three points were: at the first point - First Olfactory Neuron Point (FONP) – was 1.3 to 2.1 mm, at the second point - Middle Point (MP) was 1.1 to 1.6 mm, and at the third point – Sphenoethmoidal recess point (SERP) was 1.1 to 1.8 mm. The average in the first point was 1.78 mm, while in the second and third points were 1.41 and 1.48 mm, respectively.

Conclusion: It is concluded that the tomographic olfactory cleft reference values are respectively: at the first point – First Olfactory Neuron Point- 1.3 to 2.1 mm, at the second point - Middle Point - 1.1 to 1.6 mm, and at the third point – Sphenoethmoidal recess point -1.1 to 1.8 mm.

Key words: olfactory cleft, olfactory nose, tomographic measurements, diseases of the nose and paranasal sinuses, evo devo theory

Introduction

The olfactory cleft is classically defined as a narrow chamber located under the cribiform plate between the middle turbinate wall and the nasal septum [1-2].

There are several articles which present tomographic anatomical measurements that help the otolaryngologist surgeon to better

understand some diseases of the nose and sinuses and to get prepared for surgical procedures.
In the present study, however, we sought for a detailed anatomoradiological evaluation of the olfactory cleft that is an anatomical area of extreme relevance in the diagnosis of diseases of the nose, paranasal sinuses and olfactory disorders. An unobstructed airflow through the olfactory cleft is essential for a proper olfaction functioning. The measurement of the olfactory cleft will allow us to identify disorders in this region during the preoperative tomographic analysis, which will help us to plan the optimal treatment [9,10].
In cases where the middle meatus and olfactory fossa are opacified, encountering an enlarged olfactory fossa, as evaluated by Issa et al. with similar findings to Jankowski et al., about 47.4% of patients with nasal polyps associated with an olfactory fossa enlargement were diagnosed with sinonasal adenomatoid hamartoma (REAH) in 100% of these cases. Often underdiagnosed, to recognize the REAH is important to perform the recommended treatment that is complete resection, with rare recurrence [11-31].

According to the classical concept of nose embryology, the upper lip, nasal dorsum, septum and primary palate originate from the development of the intermaxillary process, while the lateral walls of the nasal pyramid develop from the lateral nasal processes [1,2]. It is considered that the paranasal sinuses are formed from the aeration of the facial bones by the entrance of ethmoid cells in the respective facial bones, maxillary, frontal and sphenoid, with the direction of the airflow coming from the cavity of the nose [1-3].
This description is complemented by the theory of the development of the nose and sinuses (Theory of Evolution and Development - Evo Devo), described and documented by Professor Roger Jankowski in books and scientific articles from medical journals [1-4]. Currently, this research on the evolution and development of the nose (Evo Devo) shows that the sinuses are formed from the transformation of the bone marrow from rubra to flava, with the release of nitric oxide, resulting in the formation of the air cavity - paranasal sinus - in the corresponding maxillary, frontal or sphenoid bone, with the ethmoid and olfactory cleft corresponding to a vestigial tissue that offers an explanation for a wide range of diseases of the nose and sinuses. The Evo Devo theory defines that the development of the nose can be seen as the invagination of the olfactory organ between the two maxillae toward the anterior cranial base, with the floor being secondarily formed by the appearance of a nasal breathing development at the expense of the oral cavity [1-3].

According to this knowledge, there are three different compartments in the nose: olfactory nose, respiratory nose, and paranasal sinuses. The paranasal sinuses comprise the maxillary, frontal, and sphenoid sinuses. The olfactory nose comprises the ethmoid labyrinth and the olfactory fissure, while the respiratory nose comprises all the rest of the nasal cavity below the olfactory nose [1,5-7]. According to the Evo Devo theory, it is the olfactory nose (ethmoid and olfactory fissure) that represents the seat of most diseases of the nose and sinuses.
This new way of understanding the physiology of the nose may also explain some diseases, such as nasal polyps, a reduced olfactory cleft, and the respiratory epithelial adenomatoid hamartoma (REAH) [8,11,14].
In this way, an adequate space between the septum and the middle turbinate allowing a normal airflow through the olfactory cleft is important to the passage of odorant molecules to the neuroepithelium. Considering this, the measure of a narrow olfactory cleft is important to recognize a possible cause of an olfactory disability in a clinical and radiologic review and allows us to implement the treatment in a surgical procedure gently performing a lateral luxation of the middle turbinate and decompressing the olfactory cleft and treating quantitative and qualitative reductions in the olfactory function in some patients [11-13,15,33].

Therefore, to draw the otolaryngologist's attention to the olfactory fissure, in this study we tried to determine normality values that delimit in detail the anatomy of the olfactory cleft in minimum and maximum values from a study of anatomical and radiological measurements of this area.

Materials and methods

The present study was submitted to the Research Ethics Committee of the Hospital Mater Dei (HMD) for evaluation. The study performed consists of a cross-sectional study type. The minimum required sample size for the study was estimated using a significance level of 5% (α=0.05) and a statistical power of 80% (β=0.2). To detect the minimum and maximum reference values of the olfactory slit opening in a homogeneous sample, the calculated necessary sample size was 400 CT scans of the nose and paranasal sinuses. However, 700 CT scans of the nose and paranasal sinuses requested between June 2018 and January 2022 electively at the Radiology Service of Hospital Mater Dei, Belo Horizonte, MG, were analyzed. 3700 files referring to tomographic images of the nose and paranasal sinuses were accessed, but most of these were excluded from the study for not fitting the inclusion criteria. The CT scans analyzed were taken in two CT scanners, one GE Optima multi slice 128 and the other Toshiba Aquilium multi slice 160. The images were obtained in a volumetric spiral with an axial, coronal and sagittal reconstruction.

A homogeneous group of CT scans of patients without acute or chronic paranasal sinus diseases was included in this study, seeking to define an anatomical reference measurement of the olfactory fissure. Therefore, the inclusion criterion was CT scans

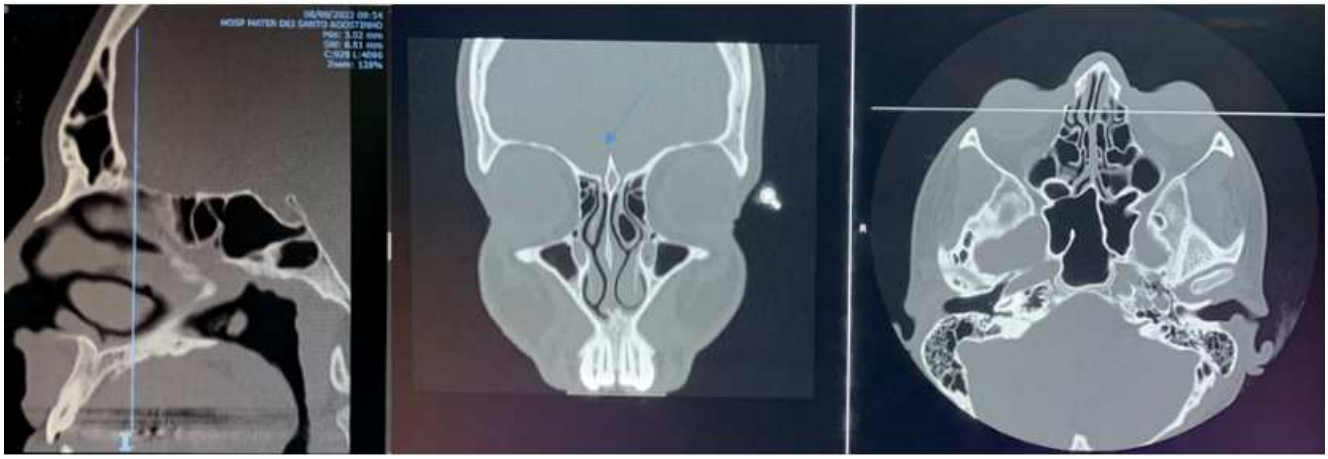

Figure 1. The first point - point of the first olfactory neuron (FONP).

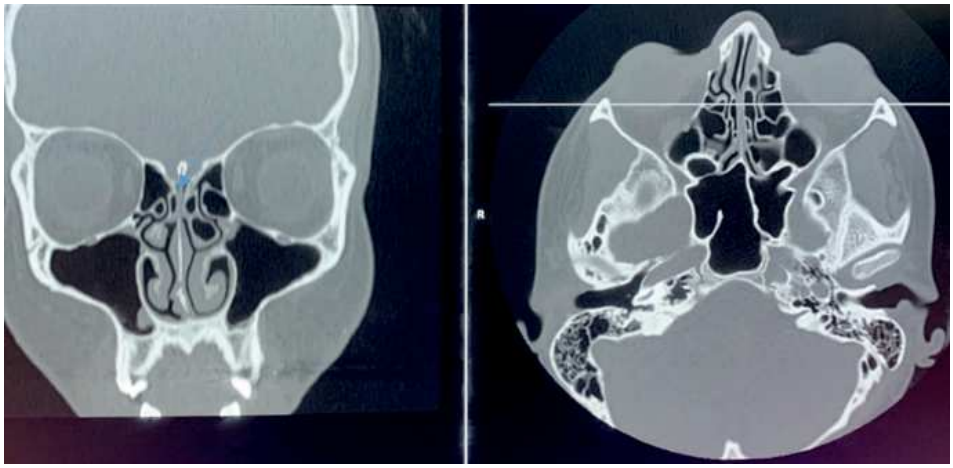

Figure 2. The second point - midpoint (MP).

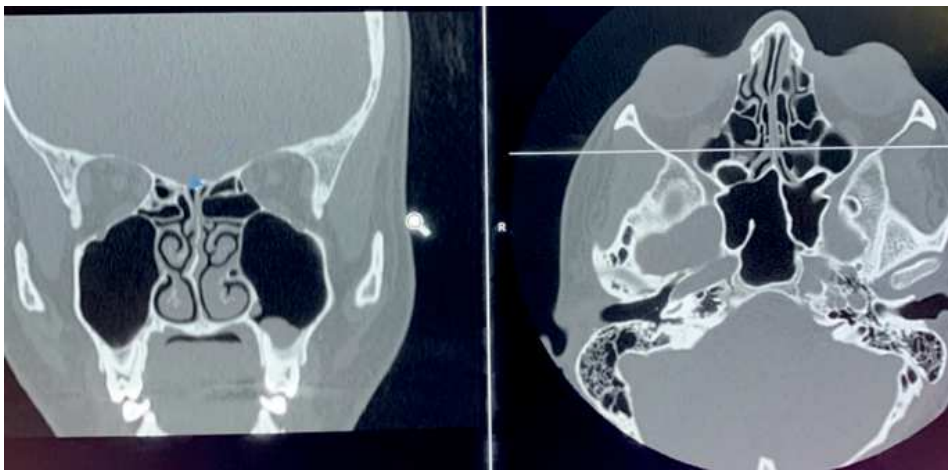

Figure 3. The third point - point of the spheno-ethmoidal recess (SERP).

of patients with anatomical changes limited to a septal deviation and/or a hypertrophy of the inferior turbinates, without changes in the middle the nasal concha, olfactory cleft or paranasal sinuses.

To obtain a CT normality criterion, CT scans requested in the emergency room for an acute disease and CT scans with evidence of a chronic sinus disease, such as chronic rhinosinusitis, nasal polyps, and hamartomas, were excluded. The CT scans were then evaluated in the coronal, axial, and sagittal planes simultaneously using the Care Stream system on three screens.

Table 1. Shows the descriptive measurements on both sides.

	M1 right	M left	M2right	M2left	M3right	M3left	Age
Mean	1,78	1,76	1,44	1,41	1,44	1,48	40,23
Standart deviatlon	0,67	0,69	0,58	0,57	0,48	0,58	16,91
Minimum	0,75	0,69	0,00	0,00	0,30	0,37	14,00
Maximum	4,90	5,27	4,56	4,82	2,83	5,86	102,00
Medlan	1,61	1,55	1,35	1,32	1,35	1,35	37,00
Percentlles 25	1,33	1,28	1,11	1,08	1,12	1,12	28,00
Percentlles 75	2,03	2,11	1,60	1,57	1,76	1,78	51,00

The measurements were then performed all on the coronal tomographic section with the aid of the other tomographic sections to identify the olfactory slit measurement points. The olfactory cleft measurements were then taken laterally between the insertion of the middle turbinate and the septum at the anterior cranial base, and on each side of the nose cavity at three specific anatomical points on the anterior cranial base Antero posteriorly, corresponding to the beginning, middle, and end of the olfactory cleft. The aim was to establish tomographic reference values of minimum and maximum normality of the olfactory slit opening in order to provide a better evaluation of the olfactory nose, in particular of the olfactory cleft.

The first anatomopathological measurement site of the olfactory cleft corresponds to the beginning of the olfactory cleft, a point that, on coronal CT scans, coincides with the beginning of the insertion (axilla) of the middle turbinate and, on sagittal CT scans, corresponds to the beginning of the lamina cribrosa of the ethmoid juxtaposed to the end of the posterior plate of the frontal sinus. This is called the point of the first olfactory neuron, because under endoscopic view it coincides with the visualization of the first fibers of the olfactory nerve (Figure 1). Note that for the identification of the first tomographic measurement point, a concomitant evaluation of the coronal and sagittal sections is necessary since the sagittal section provides an image of the beginning of the ethmoid lamina cribrosa juxtaposed to the end of the posterior plate of the frontal sinus (Figure 1).

The second site of anatomo-radiological measurement corresponds to the point located in the middle of the olfactory cleft in its anteroposterior direction, that is, between the first and the third point of the anatomo-radiological measurement. It was named the midpoint, because it is easily visible and measured after the identification of the first and third anatomo-radiological measurement points (Figure 2).

The third anatomo-radiological measurement site of the olfactory cleft corresponds to its end, which on the axial tomographic section coincides with the beginning of the appearance of the anterior wall of the sphenoid sinus, and on the sagittal and coronal tomographic sections corresponds to this same anatomical reference, i.e., the end of the ethmoid lamina cribrosa juxtaposed to the anterior wall of the sphenoid sinus. This is called sphenoethmoidal recess point, because under endoscopic view it coincides with the sphenoethmoidal recess. It is noted that for the identification of the third tomographic measurement point, a concomitant evaluation of coronal and axial sections is necessary, since the axial section provides an image of the end of the lamina cribrosa of the ethmoid juxtaposed to the anterior wall of the sphenoid sinus (Figure 3).
This detailed anatomo-radiological study of olfactory cleft normality in this homogeneous subgroup of CT scans was essential to determine minimum and maximum normality reference values for the olfactory cleft, to then use these values as a tool in the topodiagnosis of nasosinusal inflammatory diseases and associate olfactory alterations with anatomically narrowed olfactory clefts. Furthermore, the present study is pioneering in Otorhinolaryngology by determining normality reference values for the olfactory cleft.

All the measurements were taken by the same examiner. The measurements were recorded on a protocol form specifically designed for this study for a later statistical analysis.

For the data analysis, exploratory statistical techniques were used, which allowed a better visualization of the general characteristics of the data. The data were presented in tables with means, standard deviations, medians, and percentiles for the quantitative data. Continuous data were tested for the normality by the Kolmogorov-Smirnov test, and appropriate tests were used for the distribution of the data. For the comparison of continuous variables in relation to gender the T-test was used and for the association with age the Pearson correlation was used. The significance level adopted for all the analyses was 5%. The software used for the analyses was the Statistical Package for Social Sciences (SPSS) version 25.0.

Table 2. Shows the evaluation of measurements M1 to M3 on both sides according to gender.

	Gender	Mean	"Standard Deviatlon"	Medlan	P25	P75	Value p*
M1 right	F	1,82	0,70	1,63	1,35	2,03	0,184
	M	1,73	0,62	1,59	1,31	2,00	
M1 left	F	1,79	0,72	1,55	1,32	2,2	0,312
	M	1,72	0,63	1,55	1,25	2,10	
M2 right	F	1,46	0,63	1,33	1,10	1,61	0,512
	M	1,42	0,50	1,37	1,15	1,54	
M2 left	F	1,43	0,63	1,32	1,08	1,60	0,438
	M	1,38	0,48	1,32	1,09	1,56	
Ml right	F	1,44	0,50	1,35	1,12	1,74	0,802
	M	1,45	0,46	1,36	1,13	1,81	
M3 left	F	1,51	0,65	1,40	1,10	1,82	0,271
	M	1,44	0,49	1,32	1,15	1,68	

* T-test.

Results

According to the statistical analysis performed, the reference values found were: at the first point (FONP): 1.28 to 2.11 mm; at the midpoint (MP): 1.08 to 1.60 mm; and at the third point (SERP): 1.12 to 1.78 mm, which correspond to the values between the 25th and 75th percentiles at the three olfactory cleft measurement points on both sides.

The mean at the first point was 1.78 mm, while at the second and at the third points it was 1.41 and 1.48 mm, respectively. The olfactory cleft in females was larger than in males at the three points evaluated; however, the difference found between the two genders was not statistically significant.

There was no statistically significant change in the results of the minimum and maximum opening of the olfactory fossa in relation to the age of the patients (Table 1).

No statistically significant difference was found between the gender and the M1 to M3 measurements for both sides.

No statistically significant association was found between the age and the M1 to M3 measurements for both sides.
According to the statistical analysis performed, the reference values found were: in the first point - point of the first olfactory neuron (FONP) - 1.3 to 2.1 mm; in the second point - midpoint (MP) - 1.1 to 1.6 mm; and in the third point – the sphenoethmoidal recess (SERP) was 1.1 to 1.8 mm (Table 2).

Discussion

This study aimed to trace the anatomo-radiological profile of the olfactory cleft, which consists of an area of extreme relevance in the diagnosis of diseases of the nose, paranasal sinuses, and olfactory disorders. The multifactorial character of CRSs and the strict etiological uncertainty of the endotype so far make it difficult to determine the role of the olfactory fissure in upper airway inflammatory diseases and olfaction disorders.

The main objective of the present study was to evaluate a subgroup of CT scans of patients with a homogeneous character (without signs of disease in the olfactory cleft or any other suggestive of CRS). Therefore, 700 olfactory slit CT scans presenting these characteristics of normality (absence of inflammatory disease in the olfactory slit, ethmoid and paranasal sinuses) were studied. The aim was thus to define an anatomical reference measurement of the olfactory cleft to aid in the diagnosis of chronic nasosinusal diseases and to accuse the causes of a reduced olfaction, preparing an appropriate surgical or clinical therapeutic response and establishing a more assertive treatment in the olfactory cleft. Furthermore, the present study is pioneering in Otorhinolaryngology by determining normality reference values for the olfactory cleft.

There are several articles that present anatomical tomographic measurements that help the ENT surgeon to better understand some diseases of the nose and sinuses and to get prepared for surgical procedures. Among them there are studies about the importance of the patency of the olfactory cleft for a normal olfaction function and in cases when the olfactory cleft is narrow an adequate surgical decompression can be performed [33]. In other way when a wide olfactory cleft is found in the presence of nasal polyps, it is necessary to suspect to be the cause of

hamartomas to intend the adequate treatment during an endoscope surgery [5,11-15,30].
The normal size of the olfactory cleft also contributes to recognize olfactory changes resulting from "presbynasalis" factors, given that with the advancing age, in individuals over 60 years old, the volume of the olfactory fossa tends to increase. Volumes of some intranasal regions like olfactory cleft can also modulate the olfactory function, likely through alterations in the odorant deposition [35].

No statistically significant alteration was observed in the results of the minimum and maximum aperture measurements of the olfactory cleft in relation to the age of the patients.
This paper, therefore, aims to describe the anatomy of the olfactory cleft, which is essential for the diagnosis and the treatment planning of disorders in this region, making it possible to ensure a better quality of care for the patient. It also discusses the most frequent anatomical variations of this area. The present study was designed to draw the otolaryngologist's attention to the olfactory fissure, since the anatomo-radiological widening of the olfactory cleft may be the only preoperative evidence for HAER diagnosis in the chronic rhinosinusitis with polyps, and its narrowing may be the only cause for quantitative and qualitative olfactory function reductions in some patients [11-13,15].

Lima et al. [27] propose that the olfactory fissure should be considered enlarged when above 4.2 mm (when the measurement is taken from the left middle concha to the right middle concha), taking as a measurement the starting point of the olfactory fissure. When analyzing the unilateral value of the olfactory cleft measurement, we found a similar value to that found in the present study - 2.1 mm. The author's study was carried out by comparing the tomographic measurement of the olfactory cleft in a group of 100 patients, 15 of whom were diagnosed with nasosinusal polyposis with NASH, 36 with nasosinusal polyposis without NASH, and 49 without the disease. However, despite the similarity of the value found with that of our study for olfactory cleft measurements, this research was not specific to seek for a reference value of normality, but rather to suggest which measurement would be considered extended and representative of a sign of REAH.

Nguyen et al. [11,15] on the other hand, opined that the olfactory fissure should be considered enlarged when it exceeds 4.5 mm (measured from the left middle turbinate to the right middle turbinate), taking as a measurement the starting point of the olfactory fissure. When analyzing the unilateral value of the olfactory cleft measurement, we found a value similar to that found in our study, 2.1 mm. The olfactory cleft measurements taken on each side of the nose cavity, and at three different points on the anterior cranial base characterize a greater specificity to the present study, from the practical point of view they provides values of narrowing or widening of the olfactory cleft in specific locations, allowing the diagnosis of pure hamartomas for example.

Veiled olfactory slits with measurements above 4.0 mm (measured from the left middle concha to the right middle concha) constitute a sign highly suggestive of REAH [12].
Therefore, some articles define the association of olfactory fissures as widened when they measure more than 4 mm - bilateral measurement. In parallel, when they are associated with velamentation, they represent a highly probable diagnosis of HAER, which should be evaluated with a biopsy and a histopathological confirmation [11-15,18-20,28-31].

Lorentz et al. recorded in 2012 REAH in 48% of operated patients with bilateral diffuse chronic eosinophilic rhinosinusitis [28]. In 2021, research was conducted that obtained a diagnosis of HAER in 47.4% of patients operated on with the bilateral diffuse chronic eosinophilic rhinosinusitis [31]. This group of patients with the diffuse type 2 CRS associated with HAE needs to have the olfactory-nose-ethmoid and the olfactory cleft very well operated, because the HAE if not extirpated from the olfactory cleft will not respond to topical anti-inflammatory or immunobiological drugs satisfactorily [13,14,18-20,27-31,32].

According to the aforementioned articles, the olfactory cleft dilation and the olfactory cleft opacification suggest a hamartoma. Olfactory clefts with a width greater than or equal to 4.5 mm between the right and left lateral limits of the middle turbinates were considered enlarged [12,15,29,31]. If enlarged and opacified, they were considered potentially affected by hamartomas [12-14,31].

With the results observed in the present study, it is imperative, therefore, to observe the olfactory cleft, since its poor visualization as a site of REAH, which is significantly associated with polyps in the middle meatus, is still frequent among otorhinolaryngologists and explains the failure of surgical, drug and immunobiological treatments [5,7,8,11-14,18-20,28,29,30,32].

The misdiagnosis and the wrong treatment of the olfactory cleft diseases compromise the patients' outcome and prognosis. Narrow olfactory gaps can be causes of surgically reversible hyposmia, so an anatomo-radiological evaluation of the olfactory fissure and quantitative and qualitative olfactory tests are extremely important to better and appropriately treat patients with anosmia-hyposmia [2,7,8,10,11,15,24-26].

According to this study of anatomical and radiological measurements, the tomographic reference values of normality for the

olfactory cleft measurements were: in the first point - point of the first olfactory neuron (FONP) - 1.3 to 2.1 mm; in the second point - midpoint (MP) - 1.1 to 1.6 mm; and in the third point - point of the spheno-ethmoidal recess (SERP) 1.1 to 1.8 mm.

Conclusions

With these results, we added an important item to the olfactory nose evaluation protocol, which corresponds to the anatomical measurements of the olfactory cleft. These reference values will allow the surgeon to more adequately recognize and treat diseases involving the olfactory cleft.

Acknowledgments

Not applicable.

Funding

Not applicable.

Authorship contribution

TS wrote the protocol. TS, LV and GF collected the patient data, TS, RG, AG, CC, analyzed and interpreted the patient data. TV and CC wrote and translated the manuscript. All the authors read and approved the final manuscript.

Ethics approval and consent to participate

The study was approved by the ethics committee by the National Research Ethics Commission through the responsible institution, Hospital Mater Dei.

Availability of data and materials

The data sets used and/or analyzed during the present study are available from the corresponding author upon reasonable request. The names of the patients whose CT scans were analyzed have not been disclosed in the articles, the remaining data sets are available in the present study.

Conflict of interest

The authors declare no competing interest.

References

1. Jankowski R, The Evo Devo origin of the nose, anterior skull base and midface. Paris: Springer, 2013.
2. Jankowski R, Revisiting human nose anatomy: phylogenic and ontogenic perspectives. Laryngoscope. 2011;121:2461-2467.
3. Jankowski R, Septoplastie et septorhinoplastie par désarticulation: Histoire, anatomie, chirurgie et architecture naturelles du nez. Paris: Elsevier Masson 2016.
4. Jankowski R, Embryology of the nose: The evo devo concept. World J Otorhinolaryngol. May 28, 2016; 6(2):33-40.
5. Jankowski R, Respiratory epithelial adenomatoid hamartoma of the olfactory clefts. Eur Arch Oto-Rhino-Laryngol. Aug. 2011; 269(3):847-52.
6. Márquez S, Pagano AS, Lawson W, Laitman JT, Evolution of the human nasal respiratory tract: nose and paranasal sinuses. Sataloff's comprehensive textbook of otolaryngology head and neck surgery. Philadelphia: Jaypee Medical Publishers 2015; 17-42.
7. Fokkens WJ, Lund VJ, Mullol J, Bachert C, Alobid I, Baroody F, et al. European position paper on rhinosinusitis and nasal polyps 2020. Rhinol Suppl. 2020; (29):1-464.
8. Anselmo-Lima WT, Sakano E. Consenso rinossinusites: evidências e experiências. 18 e 19 de outubro de 2013. São Paulo, Braz J Otorhinolaryngol. 2015; 81(Supl. 1):S1-S49.
9. Zinreich SJ, Functional anatomy and computed tomography imaging of the paranasal sinuses. Am J Med Sci 1998;361:212.
10. Mafee MF, Endoscopic sinus surgery: role of the radiologist. AJNR Am J Neuroradiol 1991;12: 855860.
11. Nguyen DT, Gauchotte G, Arous F, Vignaud JM, Jankowski R. Respiratory epithelial adenomatoid hamartoma of the nose: an updated review. Am J Rhinol Allergy. 2014;28:187-192.
12. Hawley KA, Ahmed M, Sindwani R. CT findings of sinonasal respiratory epithelial adenomatoid hamartoma: a closer look at the olfactory clefts. Am J Neuroradiol. 2013;34 :1086-1090.
13. Gauchotte G, Marie B, Gallet P, Nguyen DT, Grandhaye M, Jankowski R, et al. Respiratory epithelial adenomatoid hamartoma: a poorly recognized entity with mast cell recruitment and frequently associated with nasal polyposis. Am J Surg Pathol. 2013;37:1678-1685.
14. Rom D, Lee M, Chandraratnam E, Chin R, Sritharan N. Respiratory epithelial adenomatoid hamartoma: an important differential of sinonasal masses. Cureus. 2018;10:e2495.
15. Nguyen PL, Nguyen G, Gauchotte G, Arous F, Vignaud JM, Jankowki R. Predictors of respiratory epithelial adenomatoid hamartomas of the olfactory clefts in patients with nasal polyposis, Laryngoscope. 2014;124:2461-2465.
16. Mammoto T, Mammoto A, Torisawa YS, Tat T, Gibbs A, Derda R, et al. Mechanochemical control of mesenchymal condensation and embryonic tooth organ formation. Dev Cell. 2011; 21:758-769.
17. Floreani SR, Nair SB, Switajewski MC, Wormald PJ. Endoscopic anterior ethmoidal artery ligation: a cadaver study. Laryngoscope. 2006;116(7):1263-7.
18. Vanden S, Bossche G De Vos, Lemmerling M. A typical but underdiagnosed nasal cavity mass. J Belg Soc Radiol. 2018;102:35.
19. Lannoy-Penisson L, Schultz P, Riehm S, Atallah I, Veillon F, Debry C. The anterior ethmoidal artery: radio-anatomical comparison and its application in endonasal surgery. Acta Otolaryngol. 2007;127(6):618-22
20. Gotwald TF, Menzler A, Beauchamp NJ, zur Nedden D, zinreich SJ. Paranasal and orbital anatomy revisited: identification of the ethmoid arteries on coronal CT scans. Crit Rev Comput Tomogr. 2003;44(5):263-78.
21. Basak S, Karaman Cz, Akdilli A, Mutlu C, Odabasi O, Erpek G. Evaluation of some important anatomical variations and dangerous areas of the paranasal sinuses by CT for safer endonasal surgery. Rhinology. 1998;36(4):162-7
22. Bayram M, Sirikci A, Bayazit YA. Important anatomic variations of the sinonasal anatomy in light of endoscopic surgery: a pictorial review. Eur Radiol. 2001;11(10):1991-7.
23. Cankal F, Apaydin N, Acar HI, Elhan A, Tekdemir I, Yurdakul M, et al. Evaluation of the anterior and posterior ethmoidal canal by computed tomography. Clin Radiol. 2004;59(11):1034-40.
24. Babbel RW, Harnsberger HR, Sonkens J, Hunt S. Recurring patterns of inflammatory sinonasal disease demonstrated on screening sinus CT. AJNR Am J Neuroradiol 1992;13:903912.
25. Shapiro MD, Som PM. MRI of the paranasal sinuses and nasal cavity. Radiol Clin North Am. 1989;27:447475.
26. Som PM, Shapiro MD, Biller HF, Sasaki C, Lawson W. Sinonasal tumors and inflammatory tissues: differentiation with MR imaging. Radiology 1988;167:803808.
27. Lima NB, Jankowski R, Georgel T, Grignon B, Vignaud JM. Respiratory adenomatoid

hamartoma must be suspected on CT-scan enlargement of the olfactory clefts. Am J Rhinology. 2006;44:264-269.
28. Lorentz C, Marie B, Vignaud JM, Jankowski R. Respiratory epithelial adenomatoid hamartomas of the olfactory clefts. Eur Arch Otorhinolaryngol. 2012;269(3):847-852.
29. Kossai M, El Zein S, Wassef M, Guichard JP, Pouliquen C, Herman P, et al. Olfactory epithelial hamartoma: a new subtype of sinonasal hamartoma. Am J Surg Pathol. 2018;42:9-17.
30. Chambers KJ, Sedaghat AR, Roberts DS, Caradonna DS. Nasal obstruction and anosmia. JAMA Otolaryngol Head Neck Surg. 2013;139:851-852.
31. Issa MJ, Vasconcelos LO, Oliveira VR, Nunes FB, Cherobin GB, Guimarães RES. Prevalence of respiratory epithelial adenomatoid hamartomas (REAH) associated with nasal polyposis: an epidemiological study – how to diagnose. Br J Otorhinolaryngol. 2021;88:49.
32. Takeda T, Yanagi N, Fukasawa N, Maeda M, Omura K, Otori N. Respiratory epithelial adenomatoid hamartoma with nasal polyps affects dupilumab efficacy. Am J Rhinology. 2022:60.
33. Biacabe B, et al., Olfactory cleft disease: an analysis of 13 cases. Otolaryngol Head Neck Surg, 2004. 130(2): 202-8.
34. Vandenhende-Szymanski C, et al., Olfactory cleft opacity and CT score are predictive factors of smell recovery after surgery in nasal polyposis. Rhinology, 2015. 53(1): 29-34.
35. Worley ML, et al., Age-related differences in olfactory cleft volume in adults: A computational volumetric study.Laryngoscope, 2019. 129(2): E55-e60.
36. Soler ZM, et al., Volumetric computed tomography analysis of the olfactory cleft in patients with chronic rhinosinusitis. Int Forum Allergy Rhinol, 2015. 5(9): 846-54.
37. Poletti SC, et al., Olfactory cleft evaluation: a predictor for olfactory function in smell-impaired patients? Eur Arch Otorhinolaryngol, 2018. 275(5): 1129-1137.
38. Kohli P, et al., Olfactory cleft computed tomography analysis and olfaction in chronic rhinosinusitis. Am J Rhinol Allergy, 2016. 30(6): 402-406.

Caroline Caixeta
Department of Otolaringology
Hospital Mater Dei Santo Agostinho
Belo Horizonte
Minas Gerais
Brazil

Tel: +55(35)999078512
E-mail: carolinecaixeta2@gmail.com